J Therm Anal Calorim (2012) 108:299–306
DOI 10.1007/s10973-011-1817-x

Investigation of thermal behavior of enoxacin and its hydrochloride

Shi Jingyan · Wang Zhiyong · Liu Yuwen · Wang Cunxin

Received: 19 May 2011 / Accepted: 20 July 2011 / Published online: 3 August 2011

Abstract The thermal behaviors of enoxacin and its hydrochloride under inert conditions were investigated by TG, FTIR, and TG/DSC-FTIR. The results indicated that the thermal behavior of enoxacin can be divided into three stages, while its hydrochloride consisted of four stages. The main difference lay in the sequence of decarboxylation and decarbonylation. For the enoxacin, the decarboxylation and decarbonylation occurred simultaneously, but for its hydrochloride, the two processes occurred in turn. The reason for this was the existence of hydrochloric acid in enoxacin hydrochloride, which changed its intermolecular force. The thermal analysis kinetic calculations of their first two stages were carried out, respectively. The apparent activation energy, pre-exponential factor, and the most probable model function were obtained using the master plots method. The results indicated that all these stages can be described by the model of nucleation and nucleus growing.

Keywords Enoxacin · Thermal decomposition · Thermogravimetry · TG-FTIR

Introduction

Enoxacin(1-ethyl-6-fluoro-1,4-dihydro-4-oxo-7-(1-piperazinyl)-1.8-naphthyridine-3-carboxylic acid, $C_{15}H_{17}FN_4O_3 \cdot 1.5H_2O$) is one of quinolone medicines of the tertiary era. It is characteristic of strong microorganism resistance, low toxin, and prominent clinic effect. The applications of enoxacin in the medicine field have been reported largely [1–3]. But the thermal induced process of enoxacin, which plays an important role in estimating expiration date of medicine and quality monitoring, was reported rarely. Though several literatures have reported the thermal behavior of enoxacin [4–6] and its metal complexes [7], due to adopting only thermal analysis technique and the single heating rate method, it is so far to describe the thermal processes in details. So the aim of this study is to investigate thoroughly the thermal processes of enoxacin and ascertain the decomposition mechanism. For this purpose, the TG-FTIR technique, which can conduct simultaneous and continuous real time analysis, is used. It can provide more information on the reaction sequences, type, and quantity of gases evolved during the decomposition process [8–10]. In addition, in present study, we used the multiple heating rate method [11] to obtain the "kinetic triple": apparent activation energy, pre-exponential factor and the most probable model function of the first two stages of enoxacin. To compare with the thermal behavior of enoxacin, that of enoxacin hydrochloride was investigated. Their generalized structures were shown below.

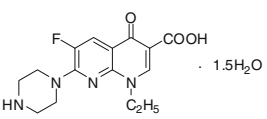

enoxacin (molecular weight 347.35)

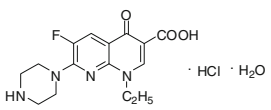

enoxacin hydrochloride (molecular weight 374.85)

Experimental

Commercially available enoxacin (Analytical Grade, Duchefa) was used without further purification.

S. Jingyan (✉)
Department of Chemistry and Environment Engineering, Wuhan Bioengineering Institute, Wuhan 430415, Hubei, China
e-mail: shijingyan@gmail.com

W. Zhiyong · L. Yuwen · W. Cunxin
College of Chemistry and Molecular Sciences, Wuhan University, Wuhan 430072, Hubei, China

TG measurements were performed on a Setaram Setsys 16 TG-DTG/DSC Instrument, France. Instrument calibration was performed with standard indium, tin, lead, zinc, silver, and gold samples of known melting temperature. All the standards were of purity >99.99%. For the kinetics measurements, about 5 mg sample was weighted into an open alumina crucible. The furnace temperature was programmed to rise from ambient temperature to 800 °C linearly at the rates of 5, 10, 15, 20, and 25 °C min^{-1}. The reaction atmosphere was nitrogen gas of high purity (≥99.999%) with a flow rate of 50 mL min^{-1}.

The TG-FTIR system composed of the Setaram Setsys 16 TG-DTA/DSC Instrument and a Thermo Nicolet Nexus 670 Fourier Transform Infrared Spectrometer. For TG-FTIR measuring, about 10 mg sample was weighed into an open alumina crucible. The heating rate of the TG furnace was 20 K min^{-1}, and nitrogen gas of high purity (≥99.999%) with a flow rate of 100 mL min^{-1} was used as carrier gas. The sample was heated from ambient temperature to 400 °C. The transfer line used to connect TG and FTIR was a 1 m long stainless steel tube with an internal diameter of 2 mm. The TG accessory of the IR Spectrometer was used, in which the 45 mL gas cell with a 200 mm path length. Both the transfer line and the gas cell were kept at a constant temperature of 200 °C. The IR spectra were collected at 8 cm^{-1} resolution, co-adding 8 scans per spectrum. This resulted in a temporal resolution of 4.32 s. Lag time that the gas products went from furnace to gas cell was about 7 s. The FTIR spectra have been identified based on the FTIR reference spectra available on the World Wide Web in the public spectrum libraries of NIST (http://webbooknist.gov/chemistry) and SADTLER Standard Infrared Spectra [12].

FTIR measurements of the pure medicines and theirs solid condensates after heated in a tube full of N_2 were carried out using a Thermo Nicolet 360 Fourier Transform Infrared Spectrometer. The data was collected at a resolution of 4 cm^{-1} in the range 4000–400 cm^{-1} using KBr pellet technique.

Theoretical

The thermal kinetic analysis was carried out by the isoconversional method and the master plots method, which had been described in details in other studies [13]. So no more description was given in this article.

Results and discussion

Thermal behavior of enoxacin

With the consideration of the lag time from furnace to gas cell, TG/DTG and the Gram-Schmidt curves of FTIR corresponding to the thermal behavior of enoxacin at the heating rates 20 °C min^{-1} were shown in Fig. 1. It indicated that the decomposition of enoxacin began at 92 °C and follows three stages (Table 1).

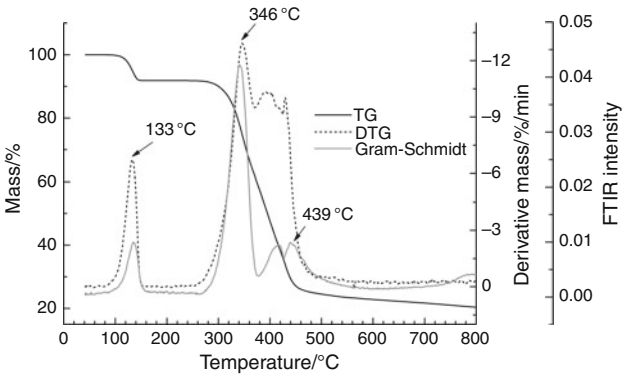

Fig. 1 The curves of TG, DTG, and the Gram-Schmidt of evolved gases at heating rate of 20 K min^{-1}, N_2 flow rate 100 mL min^{-1}

The first stage occurred at 92–151 °C and was assigned to dehydration peak. The mass percent loss was 8.06% with a molecular weight of 28.00, which was equivalent to 1.5 H_2O. The second stage was at 249–372 °C, companying the mass loss of 30.60%. The molecular weight was 106.29. The third stage represented 36.72% mass loss at 372–503 °C, which was equivalent to 127.55 by molecular weight. After 503 °C, the sample lost mass slowly. From the DTG curve, it was difficult to distinguish the second stage from third stage due to the overlap. But from Gram-Schmidt curve, the two stages can be distinguished clearly. Because the mass percent loss of the second stage and third one was very large, the decomposition mechanism was hard to be ascertained only by molecular weight.

Figure 2 is a three-dimensional diagram of infrared absorption of evolved gases versus time and wave number. It represented the change of infrared absorption at different moment and wave number. To observe and analyze expediently, we drew several absorption curves at the characteristic time out of Fig. 2 (described in Fig. 3). According to the position of characteristic absorption peak of evolved gases, seven kinds of gases were confirmed during the

Table 1 Thermal behavior data for enoxacin and its hydrochloride

Samples	Stages	Temperature range/°C	Δ*m*/%
Enoxacin	1	92–151	8.06
	2	249–372	30.60
	3	372–503	36.72
Enoxacin hydrochloride	1	80–145	3.04
	2	145–276	22.77
	3	276–388	26.67
	4	388–597	17.64

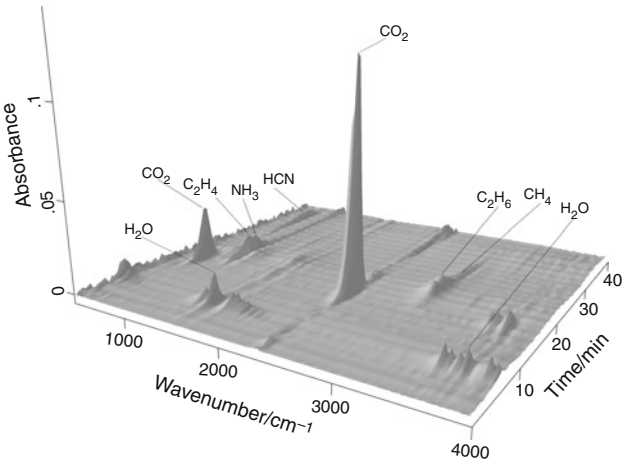

Fig. 2 The 3D surface graph for the FTIR spectra of the evolved gases produced by enoxacin (heating rate 20 °C min^{-1}; N_2 flow rate 100 mL min^{-1})

thermal decomposition: CO_2($\nu_{C=O}$ 2358 cm^{-1}); NH_3(δ_{N-H} 965, 930 cm^{-1}); HCN(ν_{C-H} 3330, 3270 cm^{-1}, δ_{C-H} 713 cm^{-1}); H_2O(ν_{O-H} 4000–3400 cm^{-1}, δ_{O-H} 2000–1200 cm^{-1}); C_2H_6(ν_{C-H} 3100–2800 cm^{-1}, δ_{C-H} 1500 cm^{-1}); CH_4(ν_{C-H} 3018 cm^{-1}, δ_{C-H} 1308 cm^{-1}); C_2H_4(δ_{C-H} 948 cm^{-1}). By plotting infrared absorption of every gas against temperature, the change of the quantity of every evolved gas with temperature can be seen in Fig. 4.

It can be seen that at the first stage, the main evolved gas was H_2O. This was consistent with the result of TG analysis. At the second stage, the main evolved gas was CO_2 accompanying the measly NH_3. At the third stage, C_2H_6, C_2H_4 and NH_3 reached the maximal release rate almost simultaneously. Ultimately, at the slow decomposition stage, CH_4 and HCN were evolved. To ascertain the decomposition mechanism clearly, we collected the solid residue under different temperatures and determined their infrared spectrum. The results were shown in Fig. 5. From Fig. 5, it can be observed that there was no absorption peak of carbonyl stretching vibration (1719 cm^{-1}) from carboxyl group in pure enoxacin, but there was absorption at 2800–2500 cm^{-1} corresponding to that of $-NH_2^+-$, which indicated that enoxacin exists in the form of betaine. This was similar to amino acid. Actually, from the point of view of molecular structure, there were one carboxy and several amidos in the molecular of enoxacin, which suggested that enoxacin belonged to amphiphatic molecule just like amino acid. So it was easy to form the inner salt [13]. And neutral quinolones had been reported existing in zwitterionic state [14]. The absorption peak at about 1629 cm^{-1} was produced by the stretching vibration of ketonic carbonyl group. At 341 °C, the absorption peak of 2800–2500 cm^{-1} disappeared, which indicated that ammonium salt had not existed. And the absorption at 1629 cm^{-1} decreased at 341 °C and disappeared at 415 °C

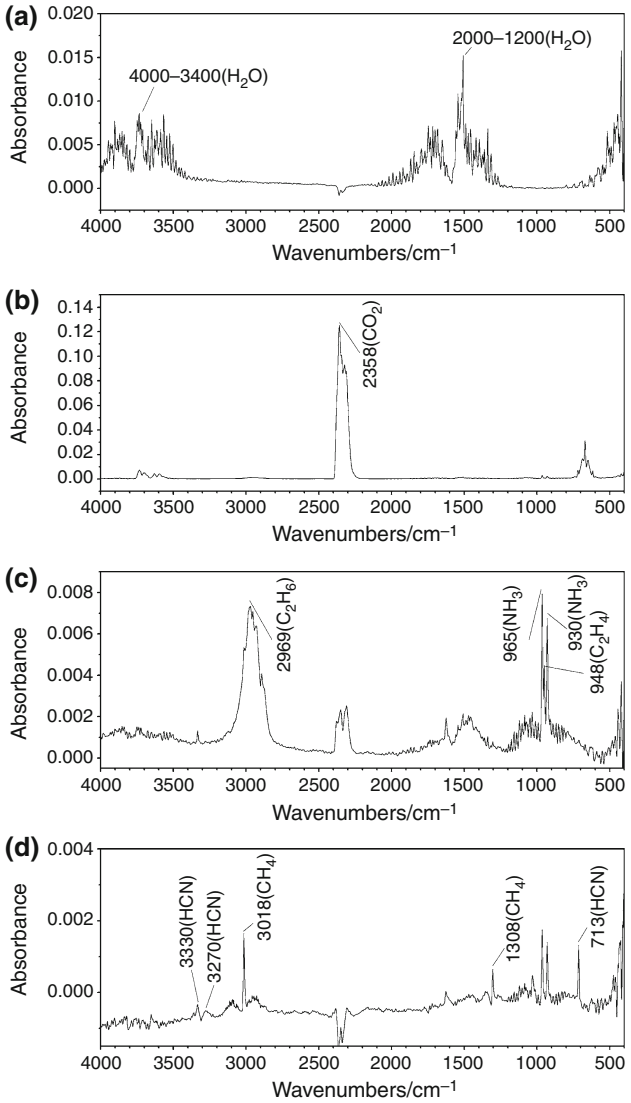

Fig. 3 The FTIR spectra of evolved gases from enoxacin decomposed in N_2 measured at different temperatures by online-coupled TG-FTIR (heating rate 20 °C min^{-1}; N_2 flow rate 100 mL min^{-1}): **a** 133 °C; **b** 343 °C; **c** 417 °C; **d** 578 °C

proved that the decarbonylation also happened in the second stage. But in this stage, no CO was detected from the evolved gas and CO_2 was the main evolved gas. It indicated that the decarbonylation reaction produced not CO but CO_2. In addition, at the slow decomposition stage, it can be seen that the solid residue was mainly saturated hydrocarbons, e.g., ν_{C-H} (2922 cm^{-1},2853 cm^{-1}) and δ_{C-H} (1381 cm^{-1}). We supposed that there existed big conjugated linkage just like graphite structure in the solid residue.

The thermal behavior of enoxacin hydrochloride

The curves of TG, DTG, and the Gram-Schmidt of evolved gases of enoxacin hydrochloride were shown in Fig. 6.

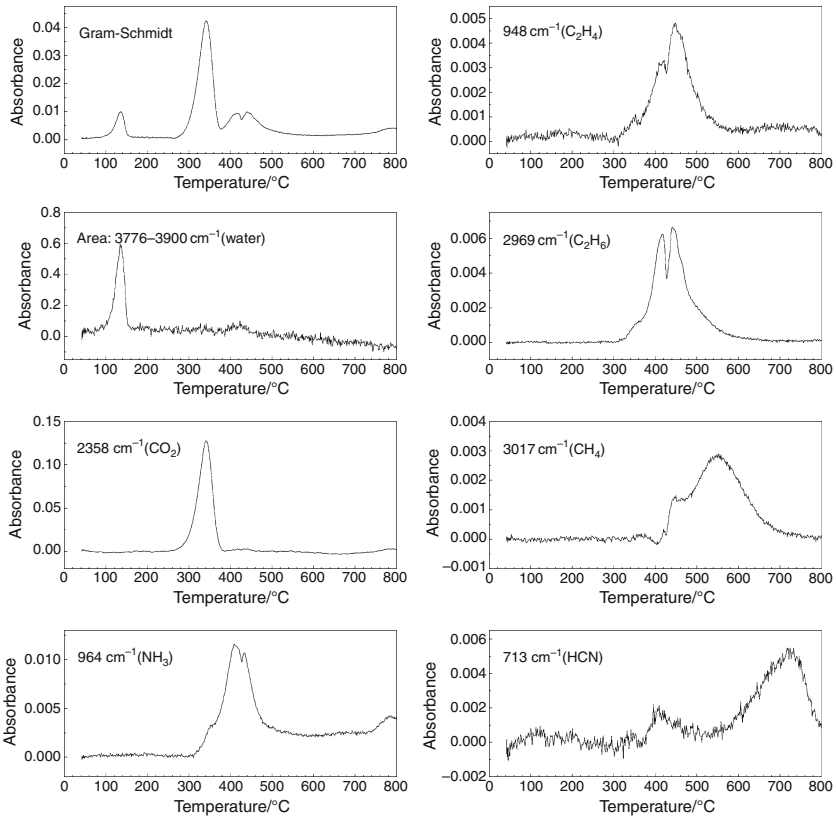

Fig. 4 IR absorbance versus temperature curves of identified evolved gaseous species evolved from enoxacin in N2, measured by online-coupled TG-FTIR system (heating rate 20 °C min^{-1}; N_2 flow rate 100 mL min^{-1})

Figure 6 indicated that enoxacin hydrochloride began to decompose at about 80 °C, which was lower than that of enoxacin. The thermal process of enoxacin hydrochloride can be divided into four stages: The first stage occurred at 80–145 °C with the mass percent loss of 3.04%. It was equivalent to 11.40 of molecular weight assigned to $0.5H_2O$; the second stage did at 145–276 °C. The mass percent loss was 22.77%, which is equal to 85.35 of molecular weight; the third stage did at 276–388 °C. The mass percent loss was 26.67% with the molecular weight of 100.08; the forth stage did at 388–597 °C. The mass percent loss was 17.64%, which is equal to 66.12 of molecular weight. According to the above analysis, it can be seen that the thermal decomposition mechanism of enoxacin and its hydrochloride was different. First, the water loss at the first

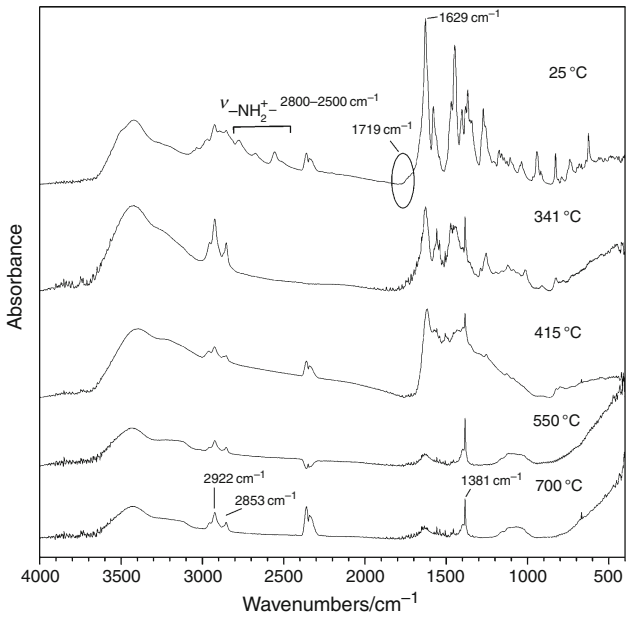

Fig. 5 The FTIR spectrum of pure enoxacin and its solid condensates in different temperatures

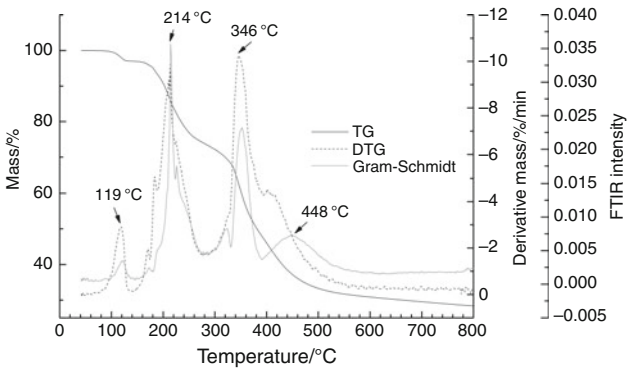

Fig. 6 The curves of TG, heat flow, and the Gram-Schmidt of evolved gases at heating rate of 20 K min^{-1}, N_2 flow rate 100 mL min^{-1}

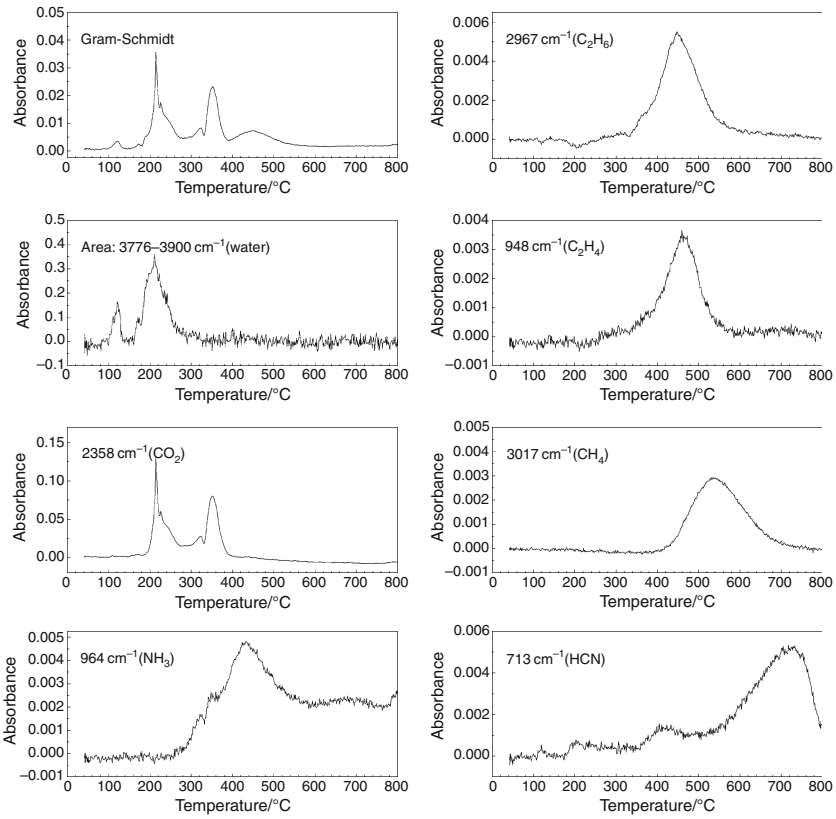

Fig. 7 Absorbance at different wave numbers versus temperature curves of evolved gases from enoxacin decomposed in N_2, measured by online-coupled TG-FTIR (heating rate 20 K min^{-1}; N_2 flow rate 100 mL min^{-1})

stage was not same. Enoxacin lost all the crystalline water, but enoxacin hydrochloride only lost part. Second, at the thermal process of enoxacin hydrochloride, a new peak appeared at about 220 °C. So the whole process added a stage than enoxacin. However, these two processes still exhibited some uniform characters. The third stage of enoxacin hydrochloride corresponded to the second stage of enoxacin. The peak temperatures of both were same. Beside this point, the ranges of temperature of both the last stages were also close. So we presumed that at the last two stages the decomposition mechanisms were same.

By analyzing several absorption curves at the characteristic time, it was obtained that the evolved gases of enoxacin hydrochloride were same to those of enoxacin. Figure 7 was the curves of infrared absorption of every gas against temperature. It indicated that at the first stage of decomposition the main evolved gas was H_2O, which accorded with the calculation of the mass loss. But the water loss was different from that of enoxacin for only 0.5 H_2O molecules lost at this stage. At the second stage, the evolved gases were CO_2 and H_2O. But in terms of the mass loss rate, it should also lost monomolecular hydrogen chloride (theoretical value is 23.88%, actual value is 22.77%). But HCl was not observed in infrared spectrum. We guessed that it maybe react with the other matter in the furnace. So it did not enter the FTIR detector. At the third stage, the evolved gas was still CO_2, accompanying measly NH_3, which was similar to the second stage of enoxacin. At the forth stage, the main evolved gases were C_2H_6, C_2H_4, and NH_3, which was the same as the third stage of enoxacin. These just proved our suggestions that the decomposition of the last two stage of enoxacin and its hydrochloride maybe same. By calculation, enoxacin hydrochloride lost monomolecular C_2H_6, C_2H_4, and NH_3 (theoretical value is 20.10%, actual value is 17.64%). At the slow decomposition stage, the evolved gases were CH_4 and HCN, which is the same as that of enoxacin.

To ascertain the decomposition mechanism clearly, we also collected the solid residue under different temperatures and investigated their infrared spectrum shown in Fig. 8 (the infrared spectrum of 25 °C is that of pure enoxacin hydrochloride). It can be seen that there existed the absorption peak of carbonyl stretching vibration (1719 cm^{-1}) from carboxyl in pure enoxacin hydrochloride, but this did not appear in pure enoxacin. The reason for this was the hydrogen chloride in enoxacin hydrochloride made 3-carboxy existing in the form of –COOH, not –COO$^-$. In addition, hydrogen chloride can linked –NH– to form ammonium salt, which can be proved by the absorption peak at 2800–2500 cm^{-1}. It can be observed that the absorption peak of carbonyl in –COOH at 250 °C had been very weak and disappeared at 352 °C. It suggested that the decarboxylation was main reaction in the second stage of the thermal behavior. This was similar to the other quinolone drugs,

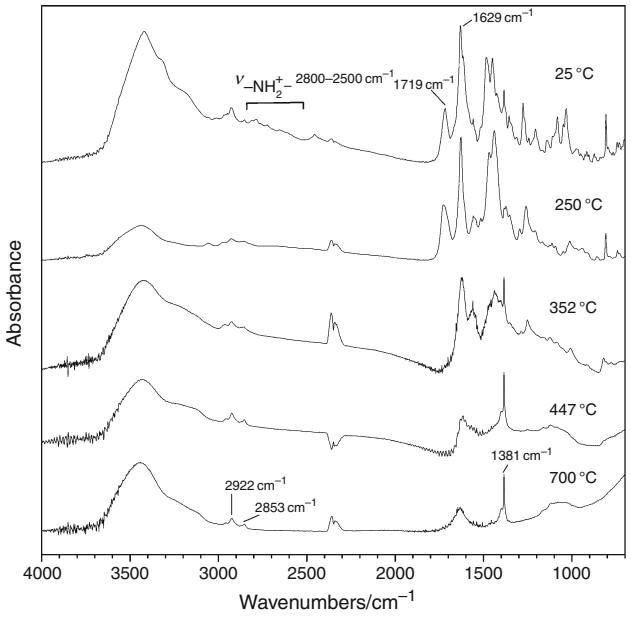

Fig. 8 The FTIR spectrum of pure enoxacin hydrochloride and its solid condensate in different temperatures

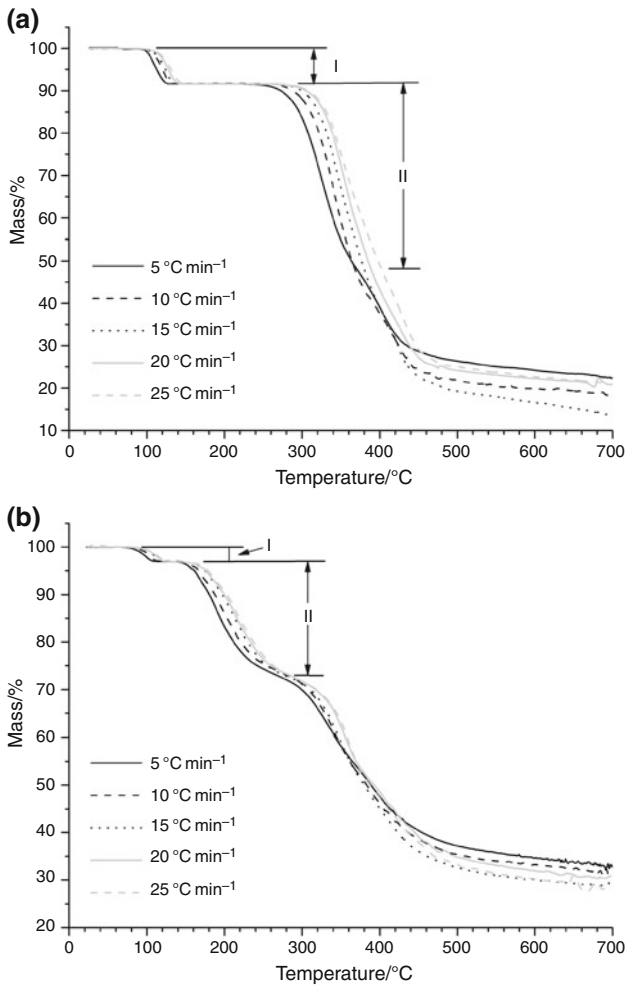

Fig. 9 TG curve of enoxacin (**a**) and enoxacin hydrochloride (**b**) at heating rates of 5, 10, 15, 20, and 25 °C min^{-1}, N_2 flow rate 50 mL min^{-1}

such as ciprofloxacin [15]. And the absorption of ketonic carbonyl group ($\nu_{C=O}$ 1629 cm^{-1}) decreased at 352 °C and disappeared at 447 °C, which indicated that the decarbonylation reaction happened in the third stage. The large yield of CO_2 gases in the third stage also proved this (Fig. 7). Therefore, we presumed that at this stage the main process was the rupture of naphthalene by analyzing the molecular structure. According with enoxacin, at the slow decomposition stage the solid residue was mainly saturated hydrocarbons. Since the decomposition temperature and productions of the third stage of enoxacin were same with the forth stage of its hydrochloride, we concluded that the mass percent loss of enoxacin at third stage should be 21.59%, namely 75 by molecular weight. Further, the mass percent loss at second stage should be 45.73%, namely 159 by molecular weight. While they were discrepant with the previous results from Fig. 1 that the mass percent loss at the second stage was 30.60% and that at the third stage was 36.72%. The reason causing this error was the gross overlap between the second stage and the third stage of enoxacin decomposition. So sometimes to ascertain the mass loss for the decomposition process only by the thermogravimetric curve was not reliable.

form of inner salt and the hydrogen from –COOH linked –NH– from piperazine to form $–NH_2^+–$. When it began to decompose, crystalline water was shucked off firstly. Second, carboxyl, carbonyl of naphthalene, and piperazine were shucked off simultaneously. The total mass percent loss was 45.49% (theoretical value 45.73%), which was equivalent with 158 of molecular weight. Third, the side chain of naphthalene ruptured absolutely and produced C_2H_6, C_2H_4, and NH_3. Under the higher temperature, the fluoro pyridine ruptured. The decomposition mechanism was described as follows:

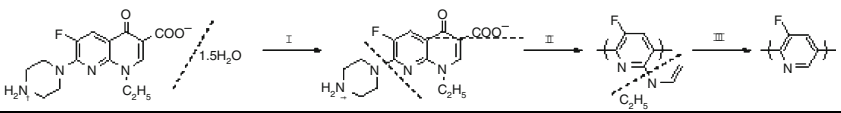

Above all, the main differences between enoxacin and enoxacin hydrochloride were the manner of decarbonylation and decarboxylation. For enoxacin, it existed in the

For enoxacin hydrochloride, the existing of chlorine hydride caused the change in the molecular structure. The imino in piperazine linked with hydrogen in hydrogen

Table 2 The thermal analysis calculation results of enoxacin and its hydrochloride

Samples	Stage	E_a/kJ mol^{-1}	$g(\alpha)$	ln A
Enoxacin	1	89.86 ± 5.83	$(-\ln(1-\alpha))^{1/2}$	23.15 ± 0.09
	2	130.32 ± 5.39	$-\ln(1-\alpha)$	20.47 ± 0.43
Enoxacin hydrochloride	1	104.33 ± 1.28	$(-\ln(1-\alpha))^{3/4}$	29.11 ± 0.03
	2	125.65 ± 5.28	$(-\ln(1-\alpha))^{2}$	26.39 ± 0.13

chloride to form $-NH_2^+-$. The carboxyl in the naphthalene existed in the form of –COOH, which is useful to form intramolecular hydrogen bond by –COOH at site 3 and carbonyl oxygen at site 4 [14]. Further, in the thermal process decarboxylation is prior to decarbonylation in naphthalene ring. And the decarbonylation in naphthalene ring occurred in the third stage companying the part of piperazine ring ruptured. Finally, the side chain of piperazine ring ruptured completely. In the higher temperature the fluoro pyridine ring ruptured. The mechanism was described below.

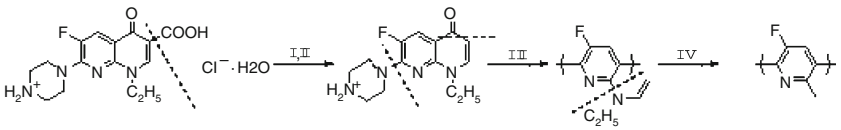

Thermal kinetics analysis

Figure 9 shows the TG curves of enoxacin and its hydrochloride at five different heating rates. To clarify the processes of the thermal behavior of enoxacin and its hydrochloride, we calculated the activation energy for each stage with TG data over the α range from 0.1 to 0.9 with an increment of 0.02 at the heating rates of 5, 10, 15, 20, and 25 °C min^{-1} by the isoconversional method. And the master plots method with forty classic heterogeneous reaction model functions [16] were used to decide the most probable model function.

From Fig. 9a, it can be observed that the mass percent loss at the first stage of enoxacin did not change with the heating rates. So it can be described by the single model function. Owing to the overlap of the second stage and third stage, it was difficult to obtain the total mass loss in the second stage directly by the TG curve. But according to the above decomposition mechanism, the limit of second stage can be ascertained clearly. Then, the thermal kinetics parameters can be obtained (in Table 2). Otherwise, for the third stage, because the mass percent loss changed with the heating rates, it cannot be described by the single model function.

For enoxacin hydrochloride, Fig. 9b indicated that the mass percent loss in its first stage and second stage did not change with the heating rates, which suggested these two stages can be described by the single model function. But the third stage and the forth stage overlapped seriously and the mass percent loss changed with the heating rates, so it cannot be described by the single model function. The thermal kinetics parameters of the first stage and second stage were calculated and listed in Table 2.

Table 2 showed the most probable model function of the first two stages of enoxacin and its hydrochloride were all similar and belonged to the model of nucleation and nucleus growing, which were often used to describe the process of formation of a new gas phase in a solid phase [17]. For example, in the decomposition process of polymer, degradation occurred accompany with melting process and inteneration, and gas produced in the inner of the sample. Our experiment was similar with this. After enoxacin and its hydrochloride were heated, they would expand into globular, and the evolved gas produced inside the sample. This proved our calculations was in consisting with the experiment result. Form Table 2, it can be seen that E_a of the second stage was bigger than that of the first stage, whether for enoxacin or its hydrochloride. It indicated that reactions of the second stage was more difficult to occur than that of the first stage, which can be seen the higher temperature was needed to induct the reaction of the second stage to occur.

Conclusions

The thermal behavior of enoxacin and its hydrochloride is discussed by TG/DTG-FTIR. The results indicated that the thermal process of enoxacin can be divided into three stages and that of its hydrochloride consisted of four stages. The reason for these was the HCl presence changed the

intermolecular force, which induced the different sequence of decarboxylation and decarbonylation.

The thermal analysis "kinetic triplet" of sublimation and evaporation processes was obtained by the isoconversional method and the master plots method, respectively. This method belongs to the method of multiple heating rates, which has higher accuracy than single heating rate in dealing with the kinetic calculation. By this method, the activation energy E_a can be obtained regardless of the reaction mechanism, which is considered more reliable.

Acknowledgements This study was financially supported by Educational Commission of Hubei Province of China (B20094006) and the research foundation of Wuhan Municipal University (No. 2008K016).

References

1. He PH, Guo DH, Zhou XQ. Current status of fourth-generation quinolone. Chin J New Drugs. 2004;13:1102–5.
2. Mehlhom AJ, Brown DA. Infectious diseases; Safety concerns with fluoroquinolones. Ann Phamacother. 2007;41:1859–66.
3. Seeger JD, Pharm D, West WA, Fife D, Noel GJ, Johnson LN, Walker AM. Achilles tendon rupture and its association with fluoroquinolone antibiotics and other potential risk factors in a managed care population. Pharmacoepidemiol Drug Saf. 2006;15:784–92.
4. Deng KJ, Luo JH. First exploration in AM1 method of quantum chemistry for mechanism of thermal decomposition of quinolone drugs. J South-Central Univ Nationalities (Nat Sci Edition). 2003;22:8–11.
5. Zhang J, Chen DH, Yuan YH, Yang TM, Qu HA. Studies on the non-isothermal kinetics of thermal decomposition of quinolone drugs and their thermal stability. Acta Pharmaceutica Sinica. 2000;35:445–50.
6. Han S, Zhu XM. Thermal analysis of norfloxacin. Chin J New Drugs. 2007;16:1104–7.
7. Badea M, Olar R, Marinescu D, Uivarosi V, Nicolesu TO, Iacob D. Thermal study of some new quinolone ruthenium(II) complexes with potential cytostatic activity. J Therm Anal Calorim. 2010;99:829–34.
8. Xie W, Pan WP. Thermal characterization of materials using evolved gas analysis. J Therm Anal Calorim. 2001;65:669–85.
9. Marsanich K, Barontini F, Cozzani V, Petarca L. Advanced pulse calibration techniques for the quantitative analysis of TG-FTIR data. Thermochim Acta. 2002;390:153–68.
10. Breen C, Last PM, Taylor S, Komadel P. Synergic chemical analysis-the coupling of TG with FTIR, MS and GC-MS: 2. Catalytic transformation of the gases evolved during the thermal decomposition of HDPE using acid-activated clays. Thermochim Acta. 2000;363:93–104.
11. Li J, Wang ZY, Yang X, Hu L, Liu YW, Wang CX. Evaluate the pyrolysis pathway of glycine and glycylglycine by TG–FTIR. J Anal Appl Pyrolysis. 2007;80:247–53.
12. SADTLER Standard Infrared Vapor Phase Spectra. Philadelphia: Sadtler Research Laboratories Inc.; 1980.
13. Shi JY, Li J, Duan Y, Hu L, Yang X, Wang ZY, Liu YW, Wang CX. Investigation of thermal behavior of nicotinic acid. J Therm Anal Calorim. 2008;93:403–9.
14. Refat MS, Mohamed GG, Farias RF, Powell AK, EI-Garib MS, EI-Korashy SA, Hussien MA. Spectroscopic, thermal and kinetic studies of coordination compounds of Zn(II), Cd(II) and Hg(II) with norfloxacin. J Therm Anal Calorim. 2010;102:225–32.
15. EI-Gamel NEA, Hawash MF, Fahmey MA. Structure characterization and spectroscopic investigation of ciprofloxacin drug. J Therm Anal Calorim. 2011. doi:10.1007/s10973-011-1584-8.
16. Li J, Wang ZY, Yang X, Hu L, Liu YW, Wang CX. Decomposing or subliming? An investigation of thermal behavior of L-leucine. Thermochim Acta. 2006;447:147–53.
17. Mamleev V, Bourbigot S, Bras ML, Duquesne S, Sestak J. Modelling of nonisothermal kinetics in thermogravimetry. Phys Chem Chem Phys. 2000;2:4708–16.